Fermilab

TM-984
1650

SATELLITE I: MODEL FOR THE SATELLITE MODE REFRIGERATOR

Henry R. Barton, Judith E. Nicholls,
and George T. Mulholland

August 12,1980

ABSTRACT

A model of the Satellite mode refrigerator has been developed to determine the refrigeration and liquefaction which can be provided by the existing cryogenic hardware, or reasonable extensions, to a series of superconducting magnets. A new FORTRAN computer program called LIQUID has been written to perform calculations using this model. This report describes a search for the optimal operating conditions of the Satellite-Central system in the Satellite mode and an examination of the effect of an extended range of operating parameters on system performance.

Realizable refrigeration as a function of temperature, Satellite and subcooler cooling curves, thermodynamic properties at the system process points, and expansion engine performance details, for a full range of Satellite compressor and Central Liquefier capacities, are reported. All solutions are constrained to a specified set of heat exchangers and a shell-side pressure drop algorithm that allows virtually unlimited flow scaling. The input parameters of the model and the text address all known influences on system performance. This report contains a selected set of compiled graphic results, and includes discussion of the model, the method and the results.

CONTENTS

1. THE SATELLITE MODE MODEL

Figure 1 is a schematic of the complete Satellite refrigerator. The process points in this report are numbered as shown in this figure.

A Satellite refrigerator can be operated in one of several modes. In the stand-alone, refrigerator mode, the gas (dry) expansion engine provides the low temperature (<40°K) refrigeration. In the Satellite mode, the flow of liquid helium FCHL from the Central Liquefier provides this refrigeration (see Figure 2). This is a study of the Satellite mode.

A set of parallel compressors is located in each sector building to provide helium at high pressure PH (atm) and room temperature T1 (°K). Six sets of these compressors feed a common manifold that supplies a high-pressure flow F (g/s) to the refrigerators. The return flow FL and the warm, lead flow FLEAD are collected in a manifold at low pressure PL. The return flow exceeds the high-pressure flow by the following amount:

$$\mathrm{FL} = \mathrm{F} + \mathrm{FCHL} - \mathrm{FLEAD}$$

A dedicated compressor returns the flow FCHL to the Central explicitly to assure that F is independent of FCHL.

The Satellite mode consumes liquid and high-pressure helium to provide its refrigeration. The mass flow imbalance by which the low-pressure stream exceeds the high-pressure stream is a parameter of paramount importance, and is defined:

$$\mathrm{BETA} = \beta = \left(1 - \frac{\mathrm{F}}{\mathrm{FL}}\right) = \left(\frac{\mathrm{FCHL} - \mathrm{FLEAD}}{\mathrm{F} + \mathrm{FCHL} - \mathrm{FLEAD}}\right)$$

The value of FLEAD depends on the Satellite location, and thus results dependent on β are often quoted for FLEAD = 0 and corrected to suit the occasion. See <u>Results</u> for detailed considerations.

The model requires a wet expander with a specified adiabatic efficiency (EFEXP2) and discharge pressure (P9), and an expander inlet heat leak (QE) and downstream, nonmagnet, heat leak (Q10). A load, Q14, that simulates real heat leaks into the cold box is uniformily distributed in the heat exchanger enthalpy (approximately uniform in T). The units of heat leak and magnet refrigeration are watts.

FCHL is a known function of β, FLEAD and F, and appears as a calculated result. The enthalpy of liquid helium delivered from the Central (HCHL) is independently specified to allow for Satellites at various distances (losses). Specification of the superheat (SDEG [°K]) of the stream returning from the magnets and a compressor efficiency (EFCOMP) (used to calculate brake horsepower requirements) complete the input requirements.

The model assumes a pressure drop of 1 atm in the high-pressure side, but scales the suction side ΔP as the 1.8 power of the flow and calculates the minimum temperature of refrigeration. The heat-exchanger capacity is scaled as the 0.8 power of the flow by special

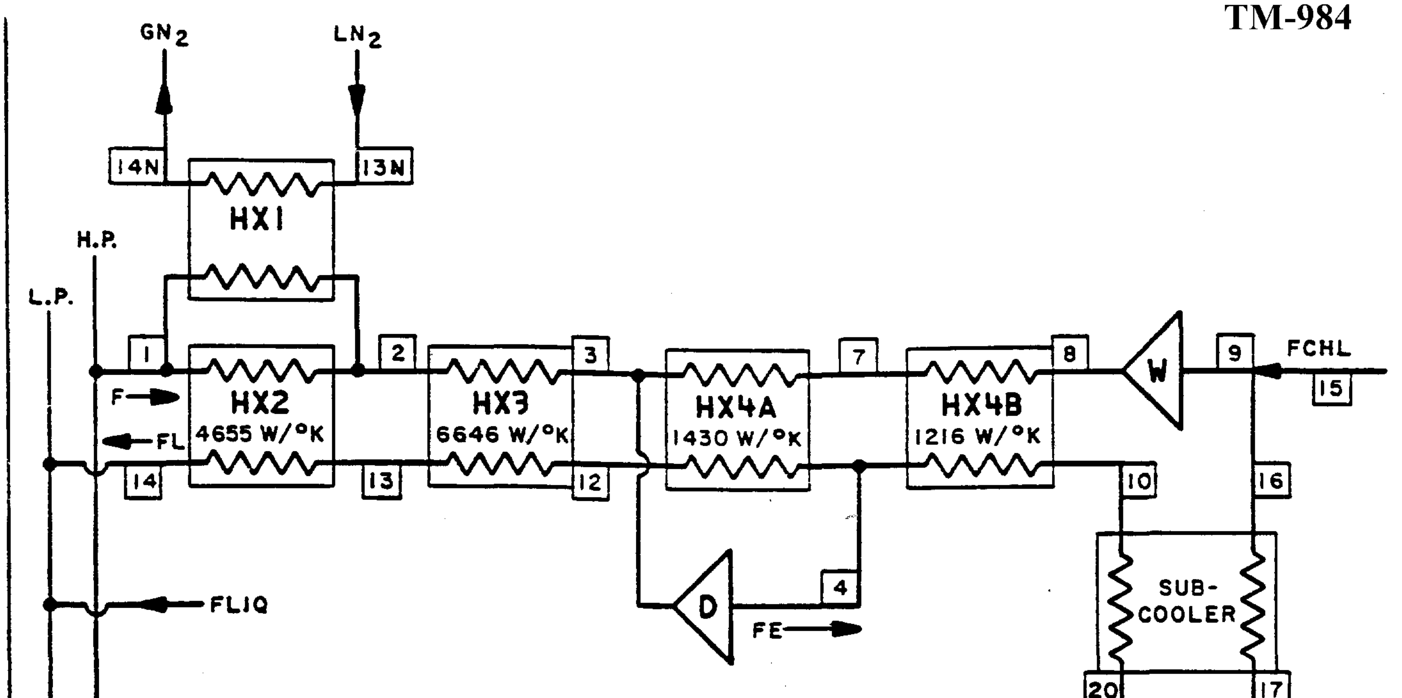

SATELLITE REFRIGERATOR
GENERAL ARRANGEMENT

FIG. 1

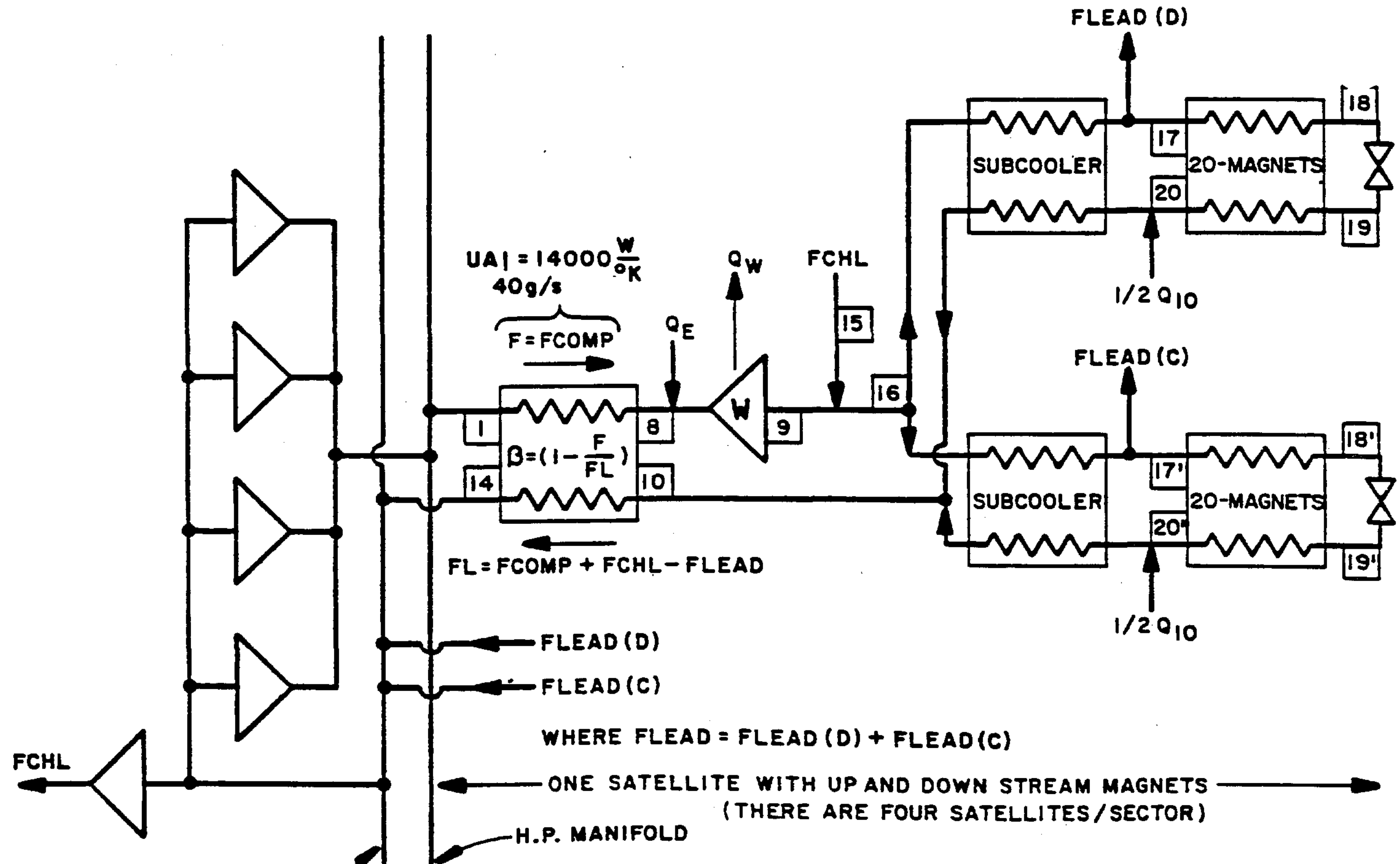

SATELLITE MODE MODEL

FIG. 2

W. CYKO 8-18-80

```
FERMILAB SATELLITE REFRIGERATOR PROGRAM
PERFORMANCE CALCULATIONS FOR A HELIUM REFRIGERATOR
THE REFRIGERATOR OPERATES IN THE SATELLITE MODE.
HAS AN ISOTHERMAL COMPRESSOR AND AN EXPANDER.


          INPUT DATA

     T1        T14         PH         PL         P9
300.000      0.000     20.000      1.030      1.800

  FCOMP     EFEXP2     EFCOMP
 50.000       .700       .750

   BETA      FLEAD       HCHL       SDEG
   .095       .960     17.470       .100

    Q14        Q20         QE
 50.000     46.000     10.000
```

Nominal Inputs -- Unless otherwise specified the nominal set of input parameters will be taken as these. T14 = 0 is a request to calculate T14.

```
                CALCULATED SYSTEM DATA

LIQUID IS SUBCOOLED.
P=      1.800 H=     11.343 T=      4.511


FRACTION LIQUEFIED BY EXPANDER      1.000

                REFRIGERATION LOADS-WATTS
                    QLOAD
                  993.776

                HEAT EXCHANGER SIZE-WATTS/K
                 16736.169

                MASS FLOW--GM/SEC
    FCOMP          F          FL        FCHL       FLEAD
   50.000     50.000      55.249       6.209        .960

                WORK-WATTS
                WCOMP

                123016.239

                COMPRESSOR HORSEPOWER =    164.901
```

procedures described in Method. This type of flow dependence is sufficient to explain the nonlinearities of Figure 3, the published specification for a popular, commercial helium refrigerator.

The model does not consider high- or low-pressure manifold pressure drops explicitly, flow in HX1, operation of the dry expander, degraded insulating vacuum, limitations on the magnitude of FCHL, F, or expander rpm and work in this study.

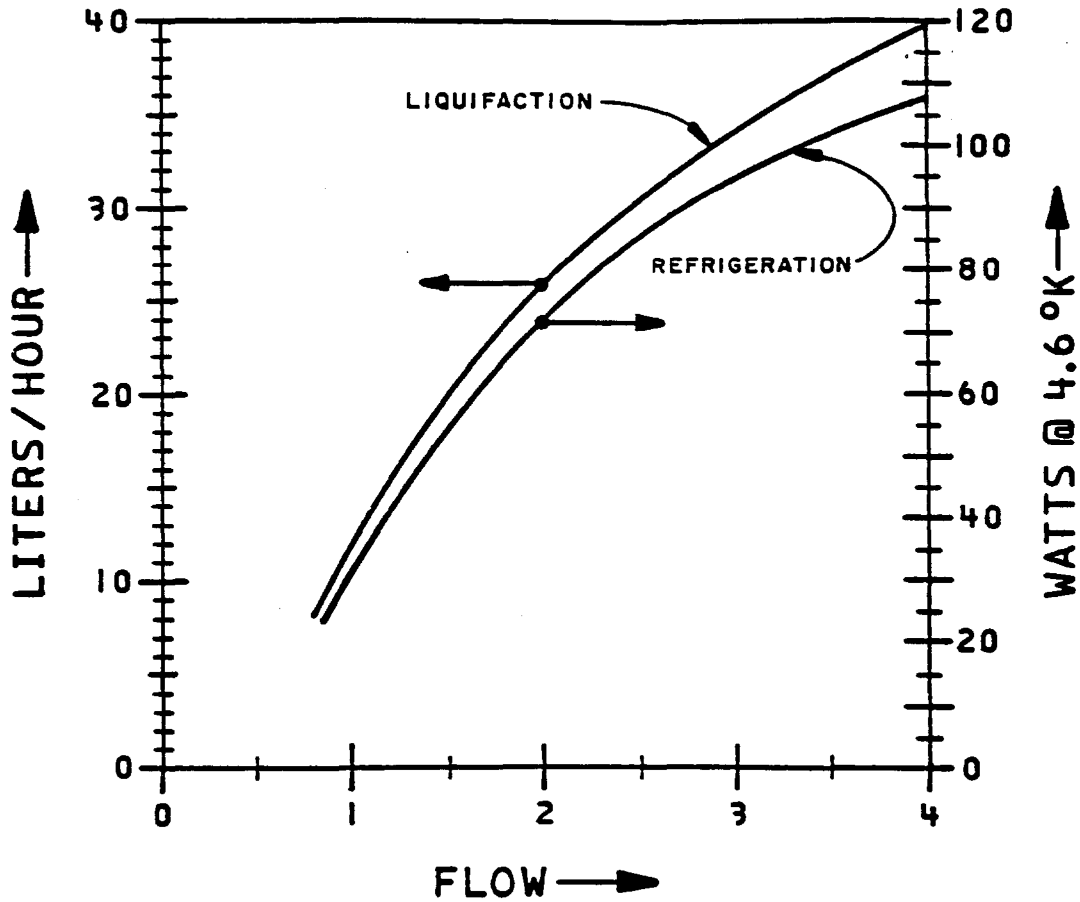

SMALL REFRIGERATOR FLOW DEPENDENCE

FIG. 3

W. CYKO 8-16-80

2. METHOD

The analysis of the refrigerator considers a closed system which is described by equations which account for the conservation of energy, momentum and mass of helium flowing in the system. In the computer program, small terms due to kinetic energy have been omitted from the heat balance. Changes in gravitational potential energy have been ignored and viscous terms have been replaced by explicit reductions in the pressure.

The Satellite refrigerator contains two-pass heat exchangers like the one shown in Figure 4. The flow in the high-pressure stream is F and this is the minimum-capacity-rate stream. The low-pressure flo is FL and the effectiveness, ε, is known for the heat exchanger. The heat exchanged between the two streams is Q. A heat balance on the heat exchanger amounts to writing the following three equations:

$$Q = F \cdot H1 - F \cdot H2$$

$$Q = FL \cdot H4 - FL \cdot H3$$

$$\varepsilon = \frac{H1 - H2}{Hi - H2},$$

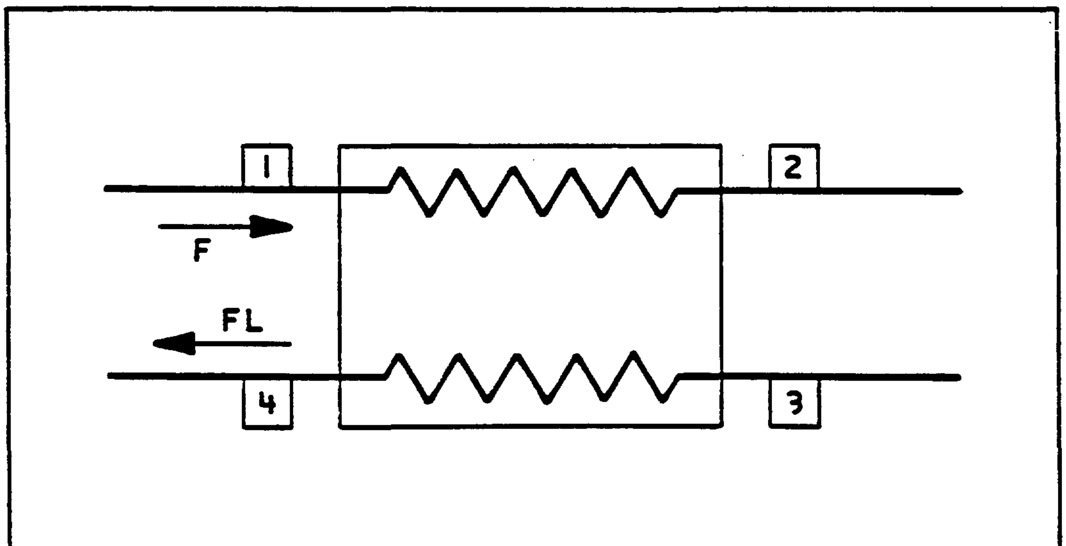

FIGURE 4. TWO-PASS HEAT EXCHANGER

The known quantities are ε, F, FL, H1, H3 and H2′, where H2′ is the enthalpy the high-pressure helium would have at process point 2 if it were cooled to the temperature T3; i.e., $\Delta T = 0$. These three equations make it possible to calculate the three unknown quantities - Q, H2 and H4. The three equations are linear relations for the unknown quantities and can be solved using matrix methods or algebraic substitution.

The expander adiabatic efficiency is specified; this allows the exit enthalpy H6 to be calculated from the inlet enthalpy H5 and known pressures (see Figure 5). Conservation of energy then requires

$$F \cdot H5 - F \cdot H6 = Q_W = \text{Engine work}$$

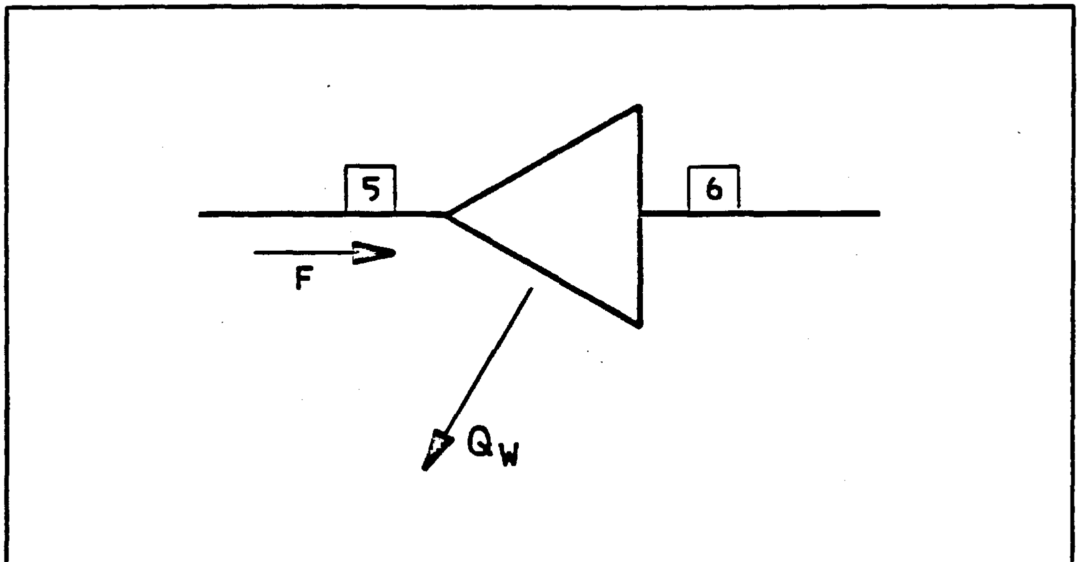

FIGURE 5. WET EXPANSION ENGINE

Heat leaks are added at the appropriate temperature levels to account for mechanical supports between cold components and room temperature parts of the cold box. A complete heat balance for the refrigerator consists of writing the equations for each heat exchanger and expander in the system. The program solves for the unknown enthalpies, the quantity of heat being exchanged in each heat exchanger and the heat being removed from the magnet load.

Several points deserve special emphasis. The simultaneous equations describing the refrigerator are linear in enthalpy, so the natural way to tackle the problem is to solve for the enthalpy at all process points. The performance of the heat exchangers and expanders is expressed in terms of efficiency, requiring a knowledge of helium properties. The adiabatic efficiency of an expander specifies the change in entropy, and requires that the corresponding enthalpies be known for helium. The correct value of the heat-exchanger effectiveness gives the UA of the existing heat exchanger; however, UA is calculated from the temperature difference between the streams in the heat exchanger. The text-book approach to the analysis of heat-exchanger performance uses an average value of the heat capacity for the process fluid. The method of analysis in the program LIQUID does not use the heat capacity of helium because it has large variations over portions of the range of operating temperature. The program does include iterative procedures to refine the accuracy of the solution in these studies. It is anticipated that the iterations will be omitted without compromising the accuracy required in future simulation work.

2.1 Heat-Exchanger UA

The Satellite refrigerators have finned-tube heat exchangers designed so that the overall heat-transfer coefficient U is dominated by the surface heat-transfer coefficient h_{tube} on the tube side. This gives the mass dependence of U as follows:

$$U \simeq h_{tube} = \frac{j\ C_p\ G}{(P_r)^{.67}} \quad .$$

Here, $j = 0.023(Re)^{-0.2}\left(1+3.5\ \frac{d_{tube}}{d_{helix}}\right)$, P_r is the Prandtl number, and d_{tube} and d_{helix} are the tube and winding diameters. Since the Reynolds number Re is proportional to mass flow and G is just the mass flow per unit cross-sectional area of the tube, the U of the heat exchanger scales as the mass flow $\dot{M}$ to the 0.8 power.

The capacity of the heat exchanger is the product of U and the area, A, available for heat transfer. The total UA of the heat exchanger in the Satellite refrigerator is specified to be 14,000 W/°K at 40 g/s mass flow so we can write

$$UA = (UA)_o\left(\frac{\dot{M}}{\dot{M}_o}\right)^{0.8} = \text{constant}\ (\dot{M})^{0.8} \quad .$$

The capacity of a heat exchanger is often given by the number of heat-transfer units N_{tu} where

$$N_{tu} = UA/(\dot{M}\ \bar{c}_p)\,, \quad \bar{c}_p = \text{average heat capacity} \quad .$$

However, because of the way the UA of a real heat exchanger depends on mass flow, N_{tu} is not a constant. The following alternate to N_{tu} is proposed in order to obtain a dimensionless parameter independent of mass flow

$$B_{tu} = \frac{UA}{\bar{c}_p(\dot{M})^{0.8}} \quad .$$

For the Satellite refrigerator B_{tu} = 138.4.

Figure 6 plots the flow dependencies of the parameters discussed; note that the product (LMDT)(UA) is directly proportional to F, a good check that nothing has been lost to the method.

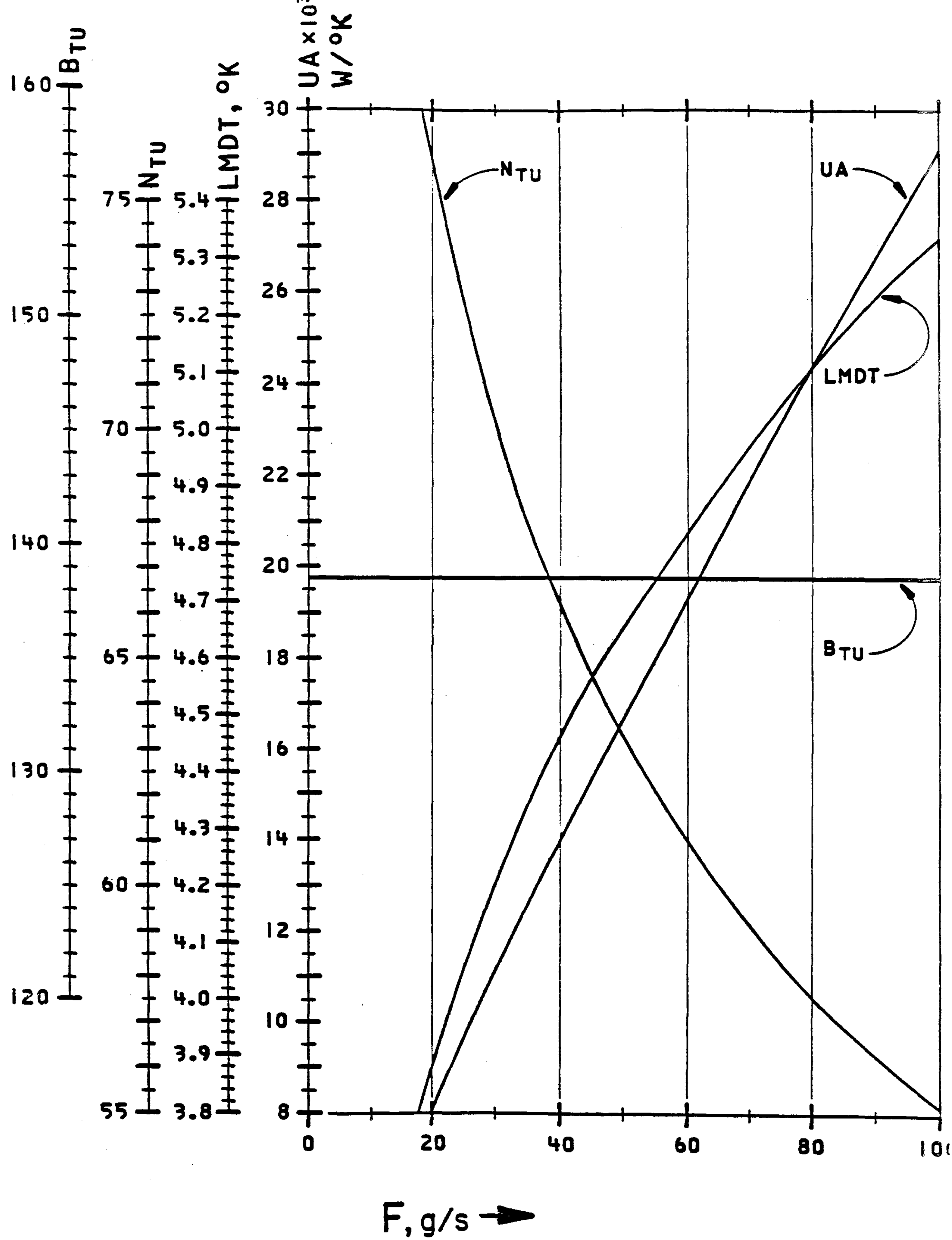

FIG. 6

W. CYKO 7-30-

2.2 Identification of the Minimum Stream

The capacity rates of the high-pressure and low-pressure streams are C_H and C_L, where $C = \dot{M}\,\bar{c}_p$. An example shows the values of C_H and C_L for F_{COMP} = 50 g/s and β = 0.075.

$$C_H = F\left(\frac{\Delta H}{\Delta T}\right)_H = (50.0\ \text{g/s})\ (1579.0 - 23.7\ \text{j/g})/(300 - 5.9°\text{K}) = 264.4\ \text{W/°K}$$

$$C_L = F_L\left(\frac{\Delta H}{\Delta T}\right)_L = (54.05\ \text{g/s})\ (1469.8 - 30.9\ \text{j/g})/(280 - 4.6°\text{K}) = 282.4\ \text{W/°K}$$

Because C_H is less than C_L in this example, the high-pressure stream is the minimum-capacity-rate stream. In a great number of cryogenic applications,[1] the low-pressure stream is the minimum stream; however, the Satellite refrigerator high-pressure stream is the minimum stream so long as β is greater than 0.02, as it is here.

The importance of identifying the high-pressure stream as the minimum stream is that it can cool to the temperature of the shell-side of the subcooler. This corresponds to the maximum possible exchange of energy between streams. The compressor suction line temperatures will, consequently, never run close to that of the compressor discharge. In fact, the suction temperature typically operates a few degrees above the water ice point.

2.3 Heat-Exchanger Effectiveness

Heat-exchanger effectiveness is defined:

$$\varepsilon = \frac{\text{actual energy transfer}}{\text{maximum possible energy transfer}}\ .$$

The maximum possible energy transfer occurs when the high-pressure stream is cooled to the temperature at the exit of the shell-side of the subcooler (T10). If H_8' is defined as the enthalpy which the high-pressure helium would have at a temperature T10, then

$$\varepsilon = \frac{H_1 - H_8}{H_1 - H_8'}\ .$$

Since ε and UA are functions of each other, specifying either fixes the other. The program uses a value for the effectiveness to calculate enthalpy H_8 at the high-pressure exit of the heat exchanger. As a check, the program calculates the UA that results from this procedure and compares it to the known UA of the heat exchanger.

The specified UA of the heat exchanger in the Satellite refrigerator is 14,000 W/°K at a flow of 40 g/s. Figure 7 shows the values of the effectiveness (solid) that correspond to the existing heat exchanger. Clearly this is a family of parabolic curves and a simple parameterization produces the dashed curves shown in Figure 3. This effec-

---

1. Barron, R., Cryogenic Systems, McGraw-Hill, N.Y. 1966.

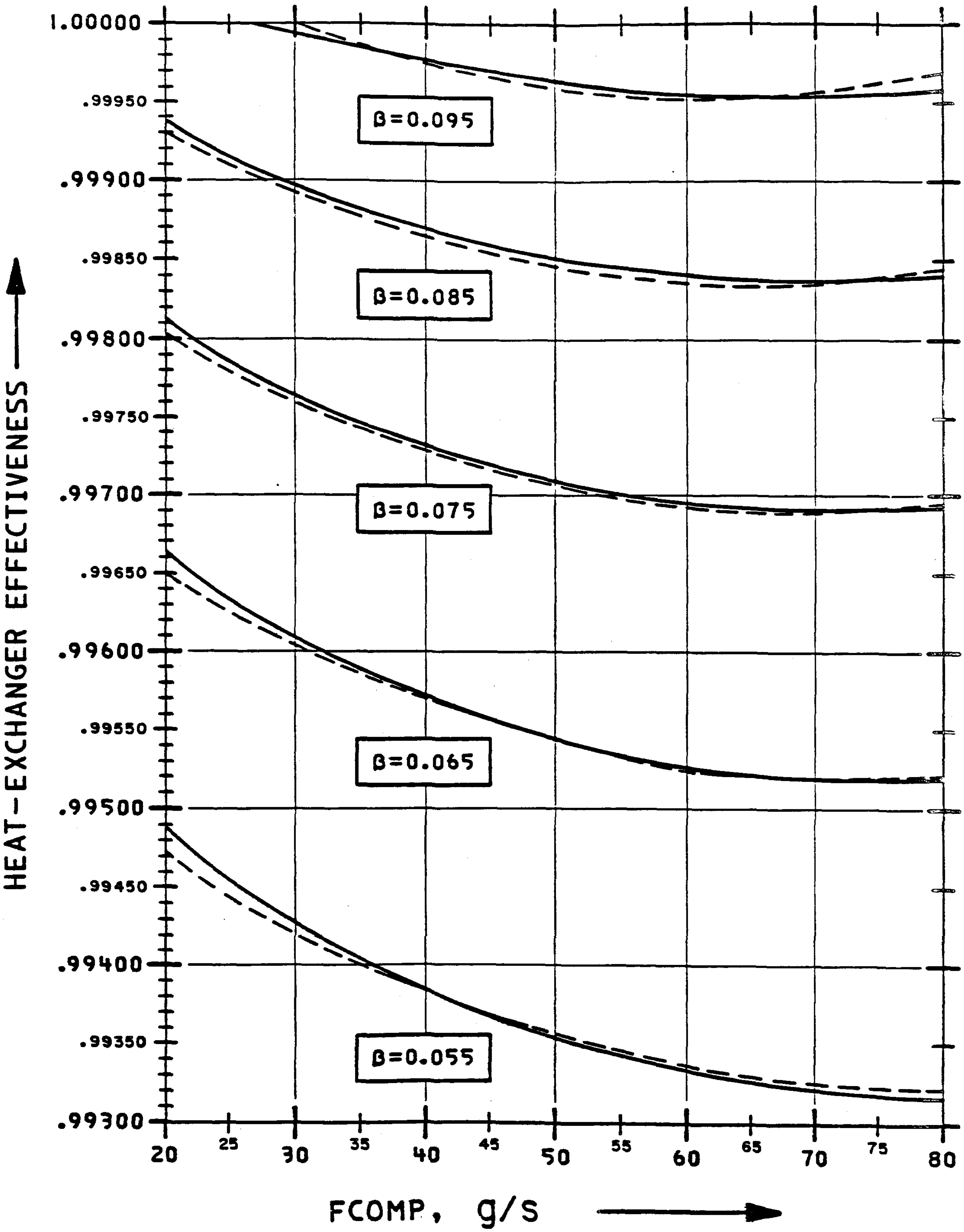

1.00000
.99950
.99900
.99850
.99800
.99750
.99700
.99650
.99600
.99550
.99500
.99450
.99400
.99350
.99300
HEAT-EXCHANGER EFFECTIVENESS
β=0.095
β=0.085
β=0.075
β=0.065
β=0.055
20
25
30
35
40
45
50
55
60
65
70
75
80
FCOMP, g/s

FIG. 7

tiveness gives a UA which is accurate to 10-20 W/°K, satisfactory for future simulations. In this report, the values of the effectiveness obtained from the parameterization initiate an iteration procedure which continues until the accuracy of UA is better than 1 W/°K. The iteration requires 5 to 10 steps to obtain this accuracy.

2.4 Shell-Side Pressure Drop

The pressure drop in the shell-side of the heat exchangers depends on the low-pressure mass flow and limits the minimum refrigeration temperature T20. The suction pressure is 1.03 atm at the compressor, and the pressure at the subcooler P20, due to all the effects in between, is

$$P20 = 1.03 + 0.195 \left(\frac{\dot{M}}{50\ g/s}\right)^{1.8} \text{atm} \quad .$$

The nominal pressure drop is taken as 1.5 times that measured,[2] and independently calculated with similar results, for the sum of the cold box exchanger pressure drops. The refrigeration temperature is obtained through the sum of the pressure drop and the manifold pressure, and the helium vapor pressure curve.

3. RESULTS

3.1 Magnet Refrigeration

Magnet refrigeration, MR, as it is used in this report, is designed to be free of qualifications; i.e., background losses have been specified and subtracted. Magnet refrigeration is available, to the last watt, to provide for the static and dynamic losses of the magnets alone.

To first order, and neglecting all detail, magnet refrigeration is dependent on two external utilities, a high-pressure flow F and a liquid helium flow FCHL. Although not immediately apparent, it is found convenient to define a ratio parameter

$$\beta = \frac{FCHL}{F + FCHL} \quad \text{(in its FLEAD = 0 form)} \quad .$$

Figures 8 and 9 display magnet refrigeration as a function of β and F respectively. The "_____ ℓ/hr" numbers labeling the FCHL curves are the equivalent Central operating rates, assuming 90% utilization.

In the flow imbalance plot, Figure 8, it is clear after a moments review of the extremes, small and large β, that F is wasted at one end and FCHL at the other, for a given level of refrigeration required. That implies an optimum of some sort between extremes. Figure 9 makes it quite clear that a rather flat magnet refrigeration maximum exists for a given FCHL; e.g., FCHL = 5 g/s, F = 60 g/s, β = 0.077, MR ≈990 watts. An efficiency optimum maximizes the ratio

2. C.Rode, see June 25, 1980 Memo to Cryo. Simulation File.

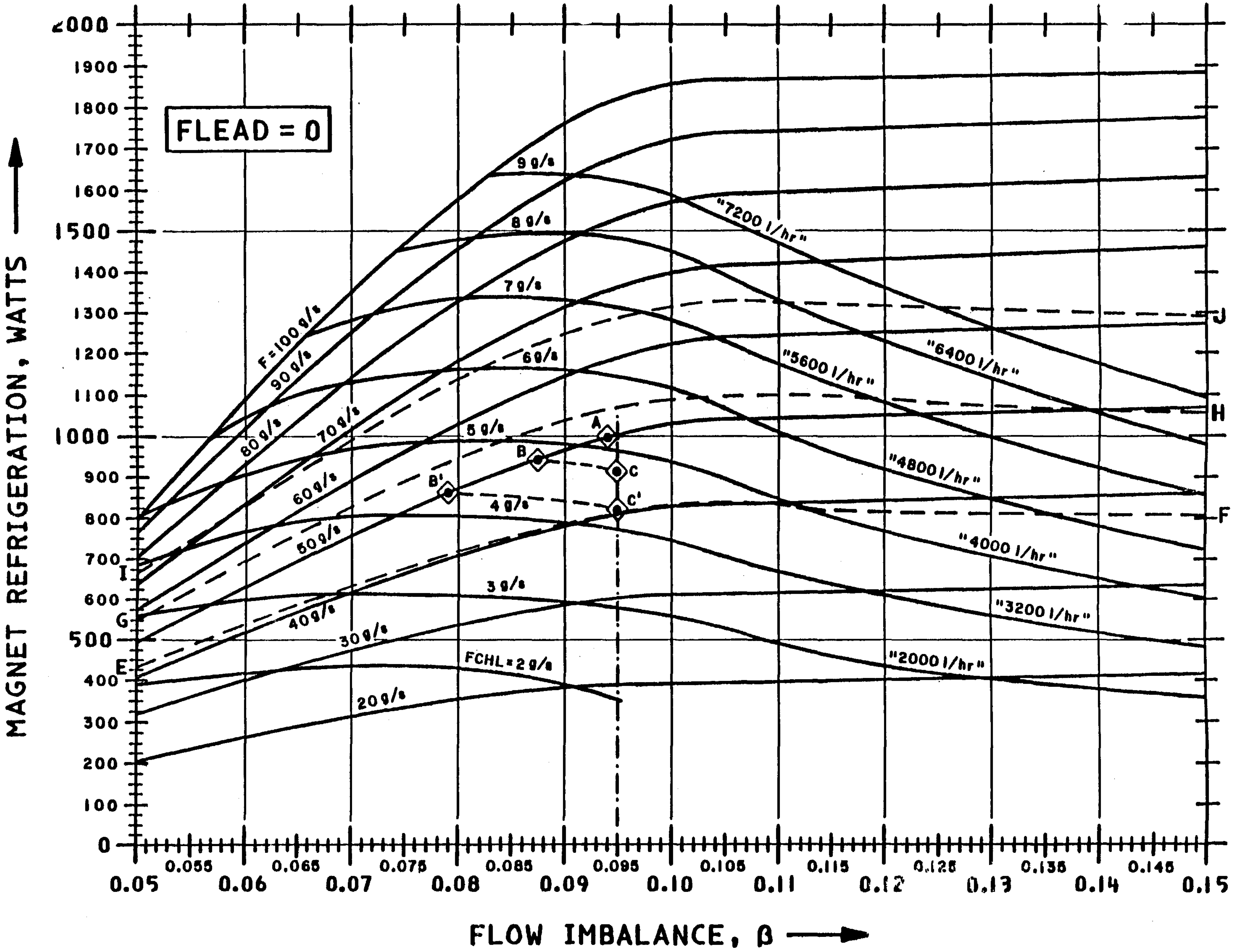

FIG. 8

W. CYKO 8-15-8(

TM-984

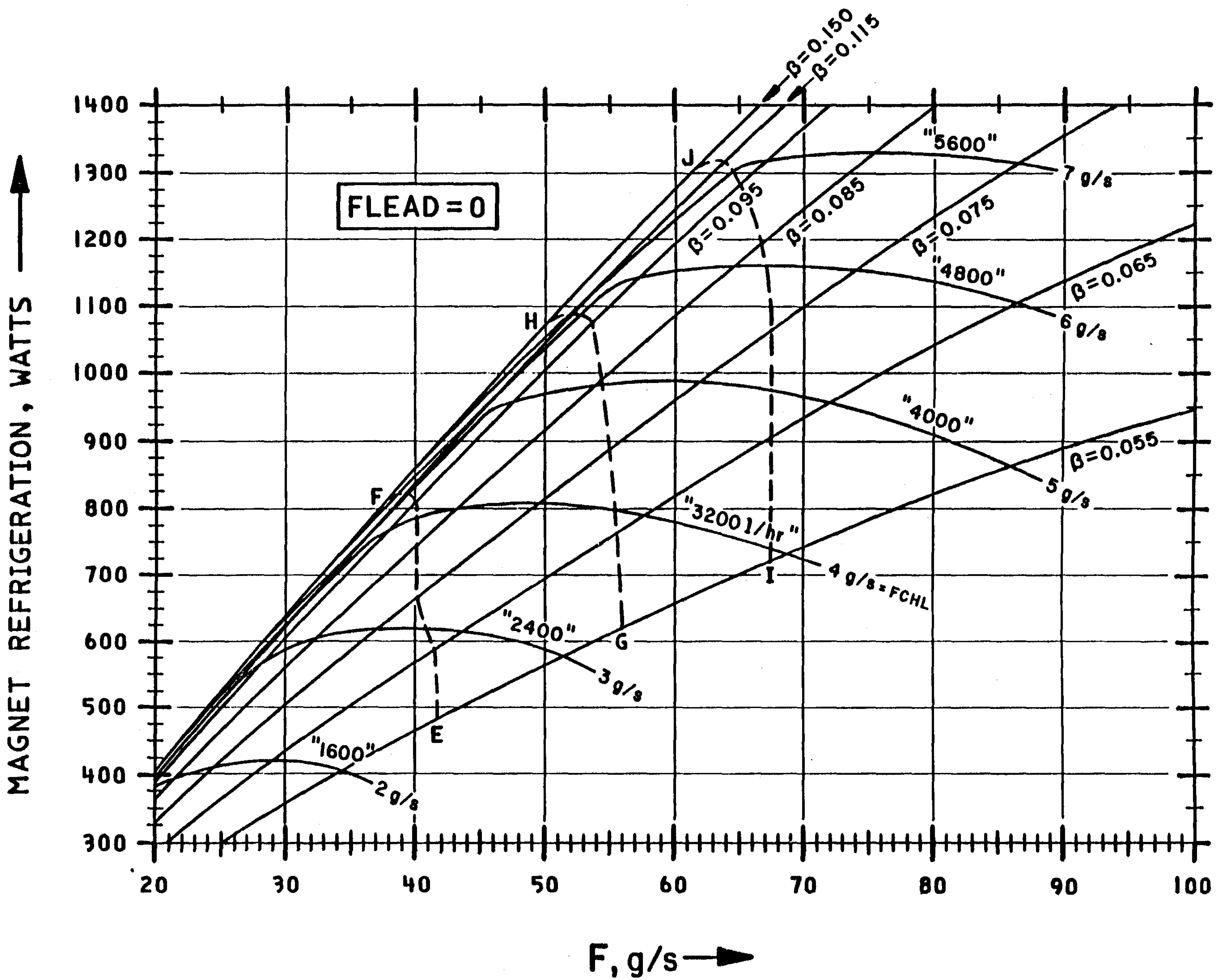
FLEAD = 0
MAGNET REFRIGERATION, WATTS
F, g/s
1400
1300
1200
1100
1000
900
800
700
600
500
400
300
20
30
40
50
60
70
80
90
100
β=0.150
β=0.115
β=0.095
β=0.085
β=0.075
β=0.065
β=0.055
"5600"
7 g/s
"4800"
6 g/s
"4000"
5 g/s
"3200 l/hr"
4 g/s = FCHL
"2400"
3 g/s
"1600"
2 g/s
J
H
F
E
G
I

FIG. 9

MR/F and results in FCHL = 5 g/s, F ≃46 g/s, β = 0.098, MR ≃950 watts.

While it is useful to investigate the MR, β, F, FCHL plane searching for better, and avoiding poorer, operating regions, the question of the temperature of delivered refrigeration is unaddressed. The same calculations that provide the results plotted in Figures 8 and 9, yield a minimum temperature of refrigeration T_R (see Figure 10 and Method for details).

The range of β from 0.055 to 0.150 has been studied, but only a representative subset plotted in Figure 10. Values of β greater than 0.095 yield magnet refrigeration values approximately equal to, or less than, the 0.095 values for a given temperature and have not been plotted. Values of F have been drawn on the figure to emphasize the connection to T_R. Note that the average temperature increase over the range 40 - 80 g/s is ≃8m°K for each g/s of return-side mass flow at β = 0.095.

It is possible to take the results T_R {MR, β} and plot an approximate locus of points of constant temperature on Figures 8 and 9. That has been done for T_R = 4.4, 4.5 and 4.6°K as the dashed curves E-F, G-H and I-J respectively. These isotherms relate minimum magnet temperature to the bolt-on horsepower (additional parallel Satellite compressor) that can usefully be employed to increase the refrigeration in this model of the existing system.

While the effect is very real it should be emphasized that this result, in particular, is very model sensitive. The authors have taken a conservative viewpoint. The model used yields a T_R 80m°K greater than the optimistic extreme, at FL = 60 g/s. Justification for the conservative view can be found in the management of the worst case flow imbalance pressure drops in the return piping.

3.2 Non-Zero Lead Flow

Six of the Satellites must provide 0.48 g/s for dipole leads and all require 0.48 g/s for the correction element leads. If we require that β and F be constant, the Central provides the necessary lead flow.

$$\text{CONSTANT} = \beta = \frac{\text{FCHL} - \text{FLEAD}}{\text{F} + \text{FCHL} - \text{FLEAD}} \Longrightarrow \text{FCHL} - \text{FLEAD} = \text{CONSTANT}$$

The effect on magnet refrigeration is, to first order, only an increased subcooler load equal to (0.96 g/s)×(H15 - H17). For anticipated values at the 24th Satellite this is approximately 5 watts. In this case the Central supplies the additional flow (current total 432 ℓ/hr) and little else occurs.

If, however, F and FCHL are held constant, a 0.48 g/s lead flow changes the operating point A to B on Figure 9. F can then be decreased with the change to point C to increase system efficiency and provide a lower T_R. Under the same circumstances, substituting B′ for B and C′ for C, describes a 0.96 g/s lead flow effect. If the Central is fully loaded and cannot provide the increased flow, the 0.96 g/s lead flow significantly (≃15%) decreases magnet refrigeration.

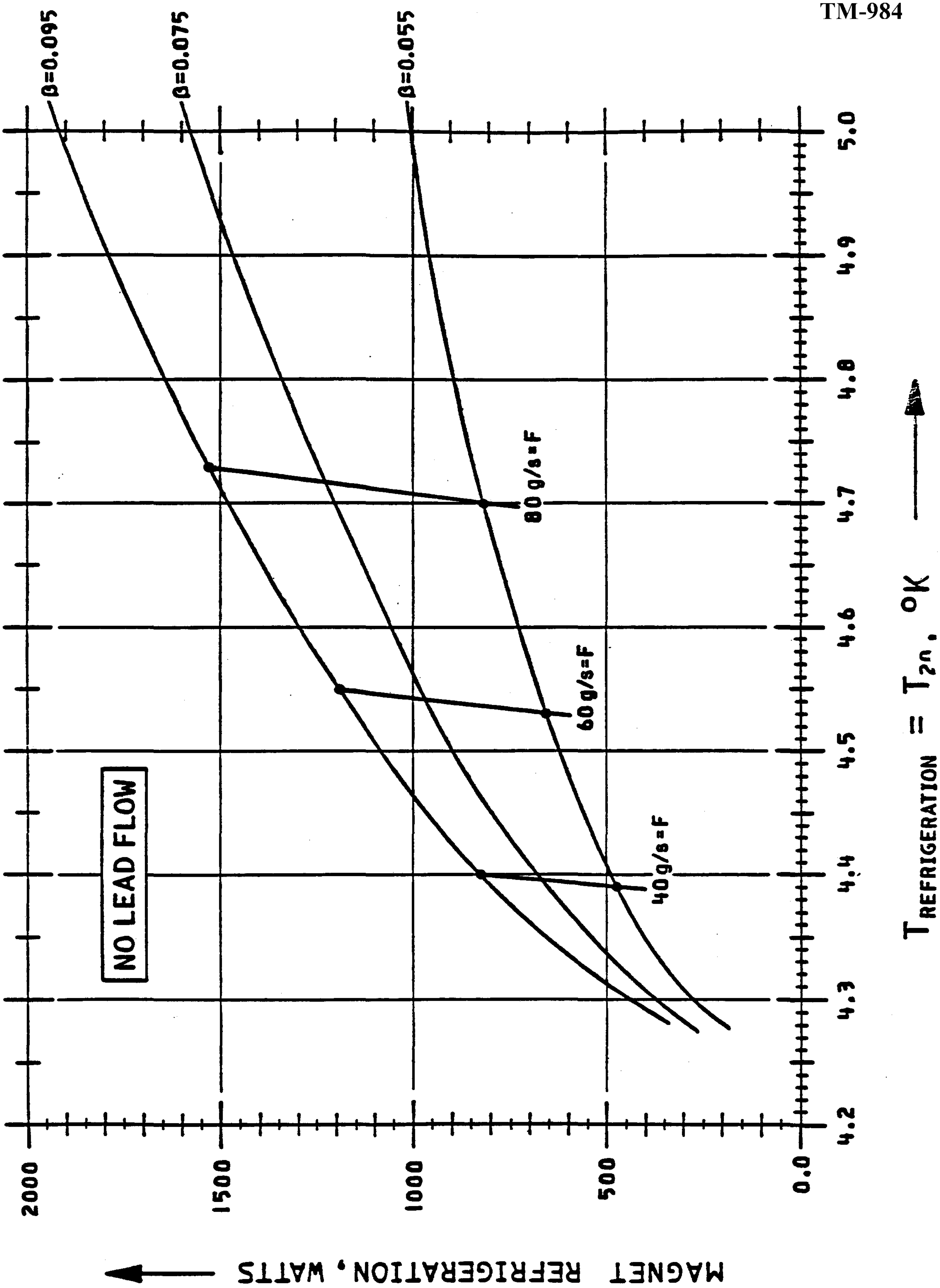
β=0.095
β=0.075
β=0.055
80 g/s=F
60 g/s=F
40 g/s=F
NO LEAD FLOW
4.2
4.3
4.4
4.5
4.6
4.7
4.8
4.9
5.0
0.0
500
1000
1500
2000
MAGNET REFRIGERATION, WATTS
T REFRIGERATION = T2n, °K

FIG. 10

3.3 Effects of Compressor Discharge Pressure

The high-pressure inlet to the refrigerator, PH, was varied from 14 to 35 atm, at F = 50 g/s, for three values of β (0.075, 0.085 and 0.095). The increased compressor work is directly related to expansion engine work (efficiency, η, taken independent of PH) and provides more magnet refrigeration to some limit in PH, as shown in Figure 11.

It is curious that the refrigeration peaks and then decreases as the engine work increases with PH. The low end ΔT (and thus β), and details of the high-pressure helium properties combine to raise the engine inlet enthalpy faster than it can extract work. Beyond about 32 atm the low end ΔT approaches zero and the effect is β independent.

The magnet refrigeration, fixed F, maximum is found at $\beta \approx 0.095$ for all PH. The efficiency and refrigeration maxima for $\beta = 0.095$ straddle the nominal 20 atm value.

The Central utilization maximum defined as MR/FCHL, occurs at $\beta = 0.075$, FCHL = 4.05 g/s, and PH = 31 atm for the data plotted. Operation at this point provides 23% more watts/unit FCHL and represents an option to increase the magnet refrigeration (+16.48%), at a cost of booster compressor horsepower (+14.7%), for FCHL = 4.05 g/s (the current example) without a concomitant increase in T_R, the temperature of refrigeration. This procedure is the only Satellite-based change that does not increase, and in fact slightly decreases, the temperature of refrigeration while increasing refrigeration.

It is important to make a clear statement of the requirements on the Central implied by Figure 11. The FCHL values that label the figure do not include a lead flow; FLEAD = 0 appears at the figure lower right. Taking 18 Satellites, each with a 0.48 g/s correction element flow, and 6 that provide a 0.48 g/s dipole flow as well, the average lead flow is 0.6 g/s. The authors believe that it will be difficult to utilize more than approximately 90% of Central production if the 24th Satellite is to be assured a continuous source of liquid helium through anticipated system perturbations. The table below summarizes these effects and concludes with the total requirement.

TABLE I

Central Liquefier Helium Requirements
(F = 50 g/s)

		β = 0.075	0.085	0.095
Actual FCHL (g/s)	FLEAD = 0	4.05	4.64	5.24
	FLEAD = 0.6 g/s	4.65	5.24	5.84
	+90% Utilization	5.17	5.82	6.49
System Total (ℓ/hr)	× 24	3,722	4,190	4,672

While all three system total requirements are under the maximum rate (4,800 ℓ/hr), two are greater than nominal rate (4,000 ℓ/hr). The conclusion scales as

$$\text{FCHL} = \left(\frac{\beta}{1 - \beta}\right) F + \text{FLEAD}$$

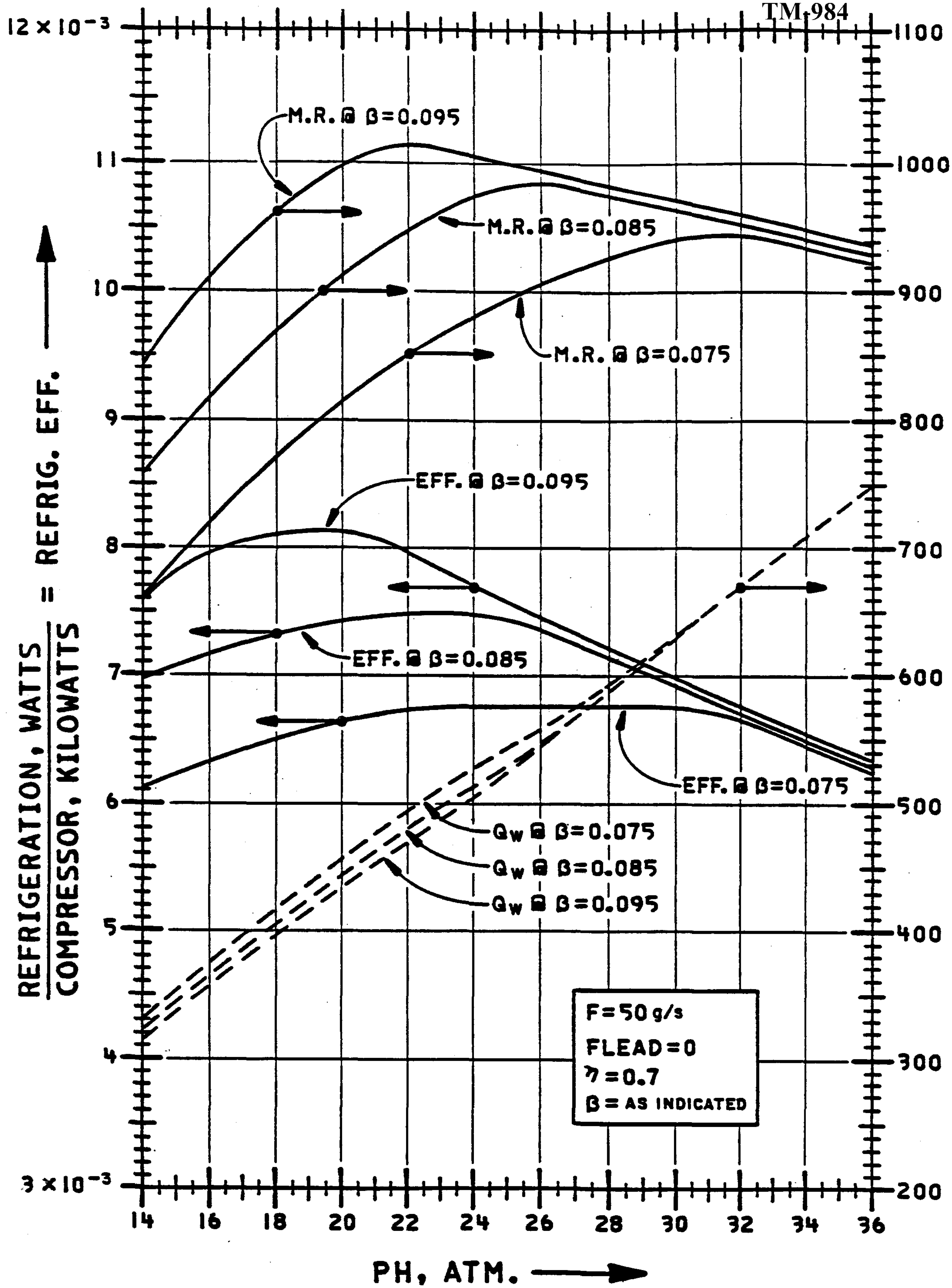

12 × 10⁻³
3 × 10⁻³
11
10
9
8
7
6
5
4
1100
1000
900
800
700
600
500
400
300
200
14
16
18
20
22
24
26
28
30
32
34
36
M.R. @ β=0.095
M.R. @ β=0.085
M.R. @ β=0.075
EFF. @ β=0.095
EFF. @ β=0.085
EFF. @ β=0.075
Q_W @ β=0.075
Q_W @ β=0.085
Q_W @ β=0.095
F=50 g/s
FLEAD=0
η=0.7
β = AS INDICATED
REFRIGERATION, WATTS / COMPRESSOR, KILOWATTS = REFRIG. EFF.
WATTS
PH, ATM.

FIG. 11

It has been noted previously that work can be extracted from the helium flow from the Central at each Satellite location by expanding it through the wet engine. This change would make up for refrigeration lost in the distribution. An adjustment of the high pressure of the Central and/or Satellites would be required. The compressor discharge pressure (greater than the current 12 atm) necessary to allow merging the flows and effect this net gain in refrigeration can be calculated from the values in the figure and the transfer line design parameters.

3.4 Expander Efficiency

The adiabatic efficiency of the wet expansion engine, η, was varied ± 0.2 about the nominal value of 0.7 to test the system sensitivity. Figure 12 illustrates the expected relationship between engine work and magnet refrigeration as a function of η and F. Less obvious is the effect of efficiency on wet engine exhaust fluid properties; the enthalpy at 1.8 atm (P9). The more interesting parameters fraction liquid and exhaust temperature, derived directly from H and P, are plotted as a function of F in Figure 13.

The fraction liquid is greatest for highest η, and decreases exponentially, beyond some value of F, because F (through its shell-side pressure drop) influences the expander inlet enthalpy. Note that these values are before the merged FCHL flow and the system subcooler. A low fraction liquid implies a significantly larger subcooler load.

The exhaust temperature is greatest for the lowest η and dramatically illustrates the variation of subcooling with η and F. Note only those regions where the fraction of liquid is 1.0 can be subcooled. The temperature 4.9°K is the two-phase equilibrium temperature for 1.8 atm fluid.

The computer output contains a page of expander specifications (see below).

The dashed line in Figure 12 describes the magnet refrigeration at $\beta = 0.095$ and the nominal $\eta = 0.7$. The change in refrigeration associated with a $\Delta\eta = 0.2$ change in engine efficiency is shown to be approximately 2/3 of the change brought about by the 26.6% increase (0.075 to 0.095) in β. It is useful to conclude that a percent loss in engine efficiency will require approximately a percent improvement in β, a requirement on the Central.

3.5 Subcoolers

The program was used to examine the refrigeration system requirements on the subcooler design. The subcooler was given a UA of 350 W/°K at a flow of 25 g/s. For these calculations, the output of the refrigerator has been divided equally between two identical subcoolers. At typical operating conditions the temperature difference between the streams is 0.09°K at the cold end, as shown in Figure 14.

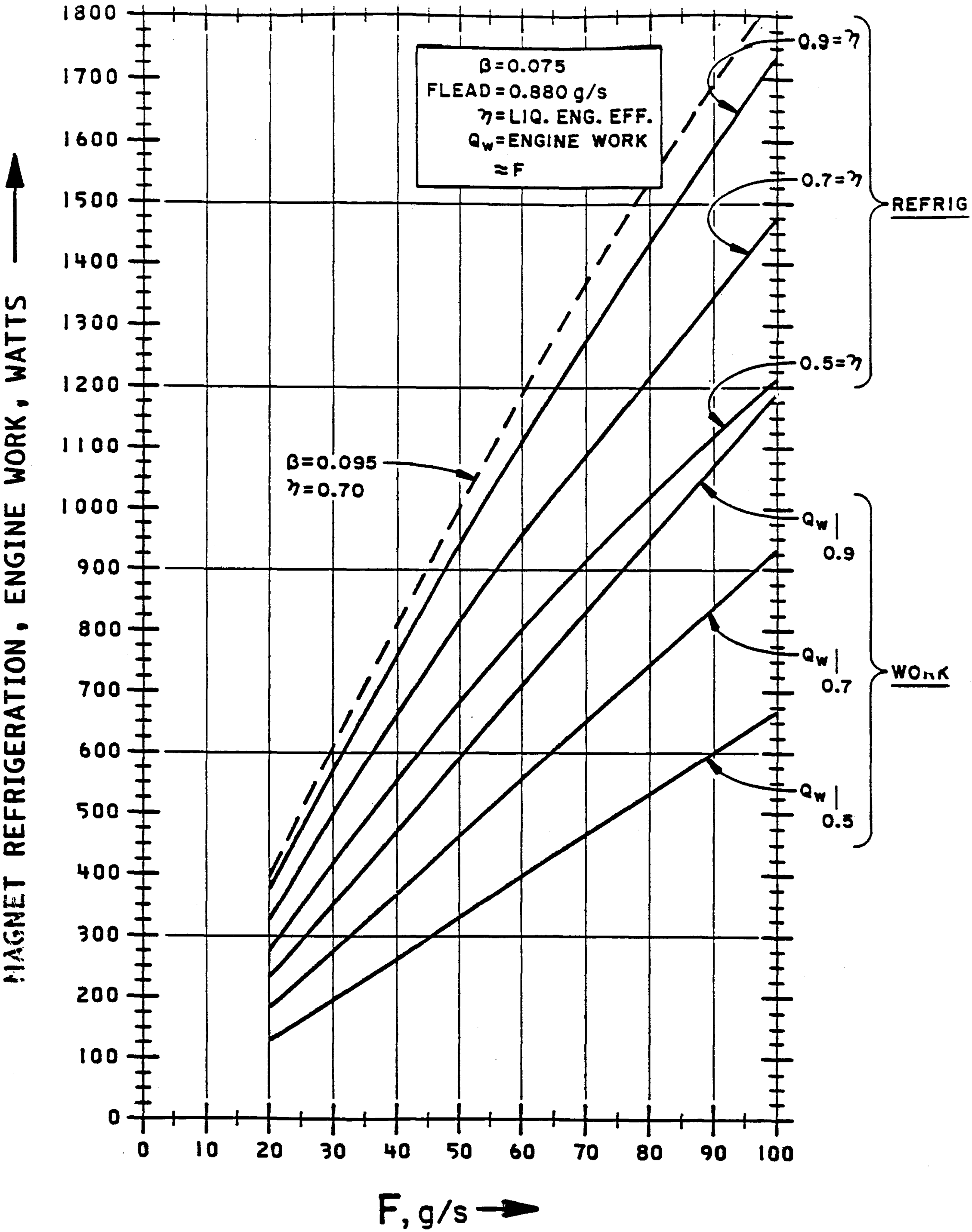

β=0.075
FLEAD=0.880 g/s
η=LIQ. ENG. EFF.
Q_w=ENGINE WORK
≈F
β=0.095
η=0.70
0.9=η
0.7=η
0.5=η
REFRIG
Q_w | 0.9
Q_w | 0.7
Q_w | 0.5
WORK
MAGNET REFRIGERATION, ENGINE WORK, WATTS
F, g/s
0
100
200
300
400
500
600
700
800
900
1000
1100
1200
1300
1400
1500
1600
1700
1800
0
10
20
30
40
50
60
70
80
90
100

FIG. 12

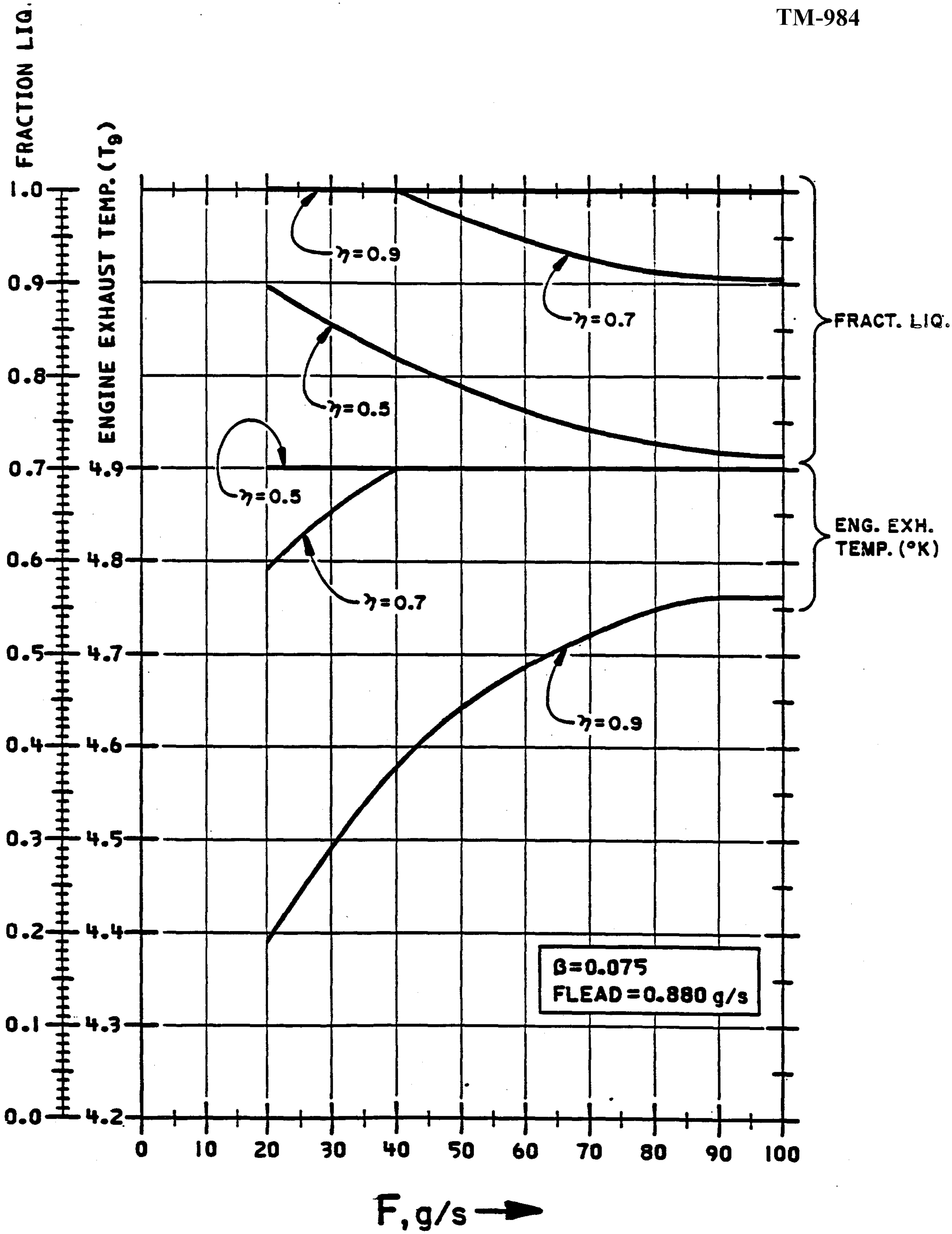
FRACTION LIQ.
ENGINE EXHAUST TEMP. (T_9)
1.0
0.9
0.8
0.7
0.6
0.5
0.4
0.3
0.2
0.1
0.0
4.9
4.8
4.7
4.6
4.5
4.4
4.3
4.2
0
10
20
30
40
50
60
70
80
90
100
η=0.9
η=0.7
η=0.5
η=0.5
η=0.7
η=0.9
FRACT. LIQ.
ENG. EXH. TEMP. (°K)
β=0.075
FLEAD=0.880 g/s
F, g/s

FIG. 13

INPUT DATA

T1	T14	PH	PL	PS
300.000	0.000	20.000	1.030	1.800

ECOMP	EFEXP2	EFCOMP
50.000	.700	.750

BETA	FLEAC	HCHL	SDFC
.375	.960	17.470	.100

Q14	Q20	QE
50.000	46.000	10.000

COOLING CURVE FOR HX5.1

HEAT TFR 1 TO 2	TEMP DIFF 1 TO 2	TEMP 1 HI PRESS	TEMP 2 LOW PRESS	ENTHALPY HI PRESS	ENTHALPY LOW PRESS	SUMMED UA
0.00	.34	4.90	4.56	15.08	30.86	0.00
4.80	.36	4.90	4.54	14.91	30.68	13.82
9.60	.37	4.90	4.53	14.73	30.50	27.00
14.40	.39	4.90	4.51	14.56	30.32	39.61
19.20	.40	4.90	4.50	14.38	30.15	51.72
23.99	.41	4.89	4.48	14.21	29.97	63.41
28.79	.41	4.87	4.46	14.03	29.79	75.23
33.59	.39	4.86	4.46	13.86	29.61	87.22
38.39	.37	4.84	4.46	13.69	29.44	99.75
43.19	.35	4.82	4.46	13.51	29.26	112.94
47.99	.33	4.80	4.46	13.34	29.08	126.86
52.79	.31	4.78	4.46	13.16	28.90	141.66
57.59	.29	4.76	4.46	12.99	28.73	157.48
62.39	.27	4.73	4.46	12.81	28.55	174.55
67.19	.25	4.71	4.46	12.64	28.37	193.14
71.98	.22	4.69	4.46	12.46	28.19	213.61
76.78	.20	4.66	4.46	12.29	28.02	236.53
81.58	.17	4.64	4.46	12.11	27.84	262.56
86.38	.14	4.61	4.46	11.94	27.66	293.01
91.18	.12	4.58	4.46	11.77	27.48	329.86
95.98	.09	4.55	4.46	11.59	27.31	376.96

AVAILABLE UA (WATTS/K) = 377.8
REQUIRED UA (WATTS/K) = 377.0
AVERAGE LMDT (K) = .255
REQUIRED NTU = 1.6

Figure 14.

EXPANDER SPECIFICATIONS		
	EXPANDER	
ADIABATIC EFFICIENCY	.700	
MASS FLOW-GM/SEC	50.000	
PRESS RATIO	10.556	
WORK-WATTS	433.562	
	INLET	OUTLET
PRESSURE-ATM	19.000	1.800
TEMPERATURE-K	4.843	4.511
ENTHALPY-J/GM	20.014	11.343
ENTROPY-J/GM-K	2.950	3.659
SPECIFIC HEAT,CP-J/GM-K	3.021	5.571
SPECIFIC HEAT RATIO,CP/CV	1.349	2.267
DENSITY-GM/CC	1.590E-01	1.229E-01
VISCOSITY-GM/CM-SEC	5.738E-05	3.173E-05

The subcooler is a heat exchanger with two-phase flows. The model of the subcooler is the one used to describe the heat exchanger in the refrigerator. The high-pressure stream of the subcooler is the minimum one. The UA of the subcooler was given an 0.8 power law dependence on mass flow.

Figure 15 shows that each subcooler will be required to transfer 10 to 200 watts of heat (Q_{sub}). The lower requirement applies at high β; in this case the output of the expansion engine is already subcooled. Figure 15 also shows the dependence of the logarithmic mean delta T, LMDT, on β. Since UA = Q_{sub}/LMDT, these two curves are nearly parallel; the deviation is due to the increase in UA when using more Central flow (higher beta).

Figure 16 shows that magnet refrigeration increases about two percent for each additional 0.1°K of superheat at the exit of the low-pressure side of the subcooler. This effect is much smaller than the increase obtained by using more flow from the Central. Operating with superheat greater than 0.4°K does not provide subcooling because the shell-side of the subcooler (and a portion of the last magnet) contain only gas.

The subcooling available at the magnets is shown in Figure 17. In the best case, about 0.4°K of subcooling is obtained. This is achieved by operating at a low superheat and a high β.

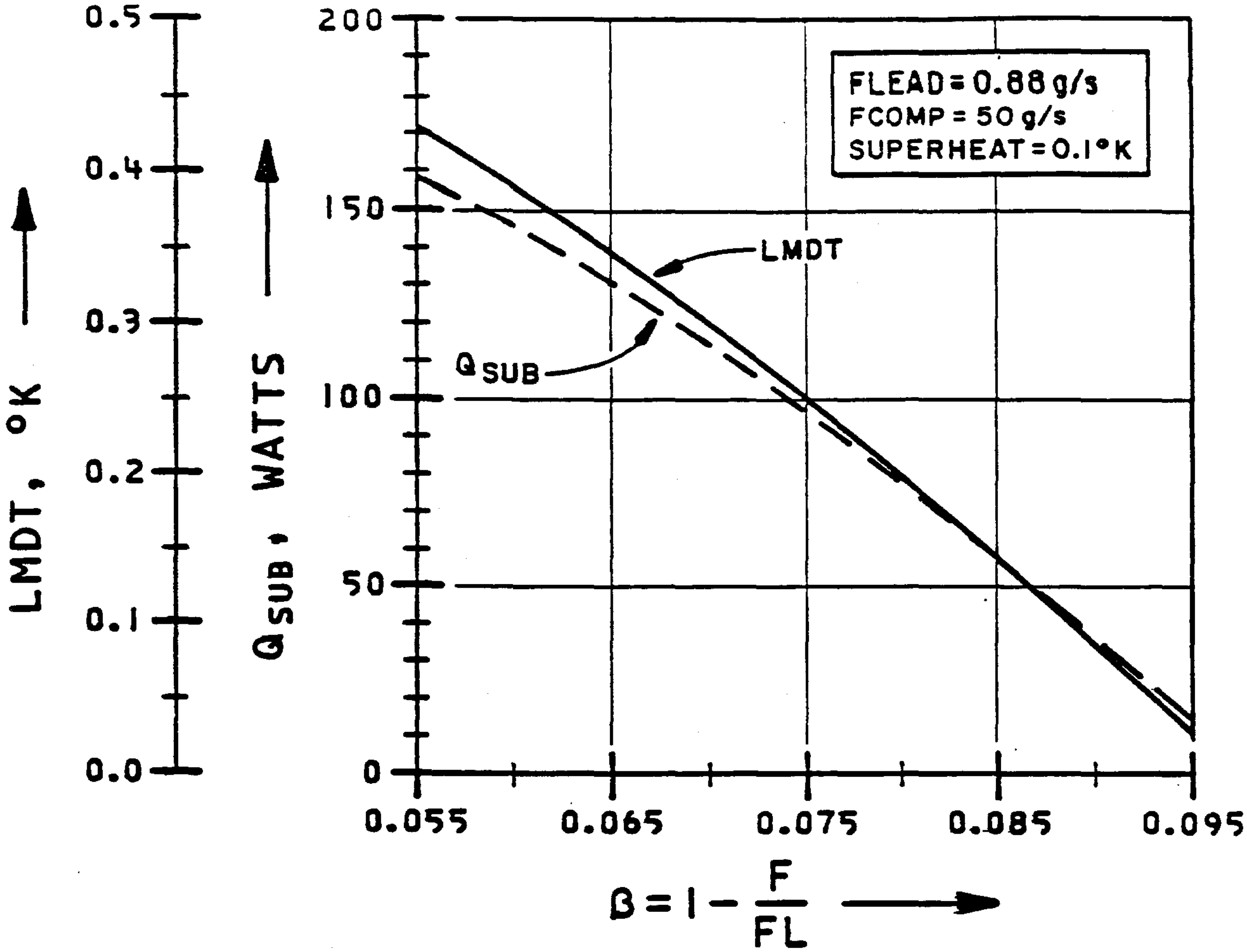

FLEAD = 0.88 g/s
FCOMP = 50 g/s
SUPERHEAT = 0.1°K
LMDT
Q_{SUB}
LMDT, °K
Q_{SUB}, WATTS
0.0
0.1
0.2
0.3
0.4
0.5
0
50
100
150
200
0.055
0.065
0.075
0.085
0.095
$\beta = 1 - \frac{F}{FL}$

FIG. 15

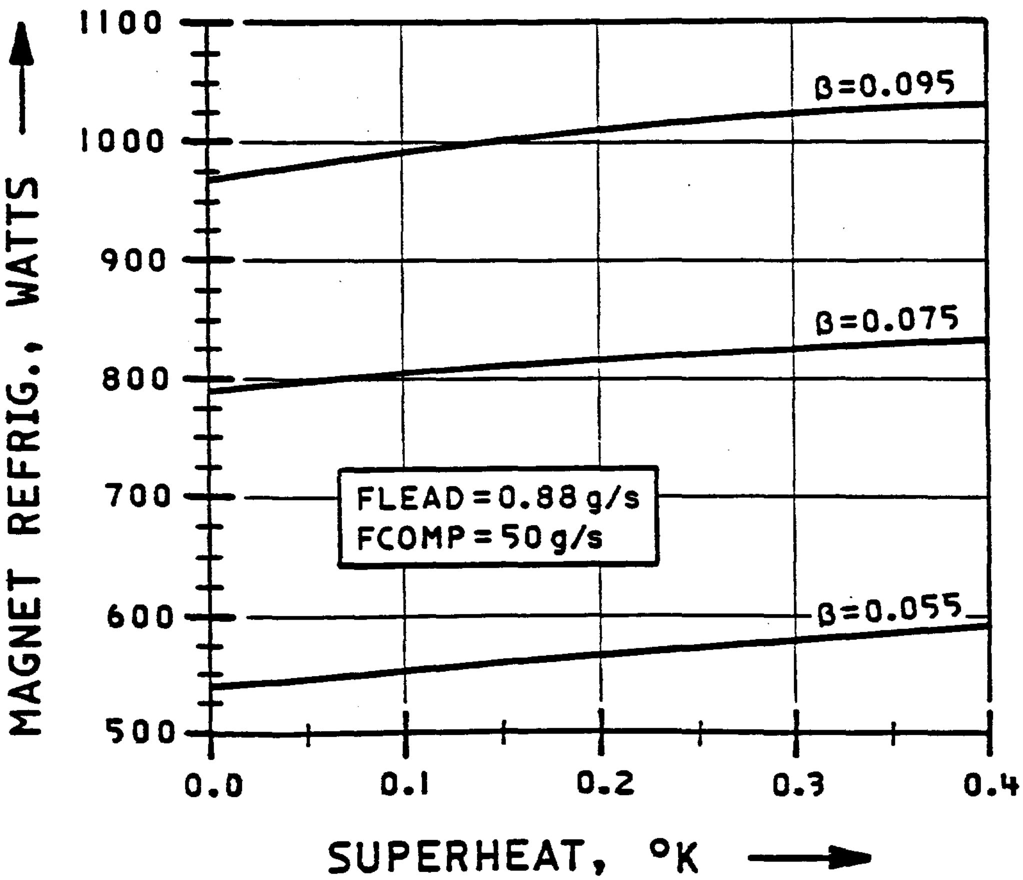

β=0.095
β=0.075
β=0.055
FLEAD = 0.88 g/s
FCOMP = 50 g/s
MAGNET REFRIG., WATTS
500
600
700
800
900
1000
1100
0.0
0.1
0.2
0.3
0.4
SUPERHEAT, °K

FIG. 16

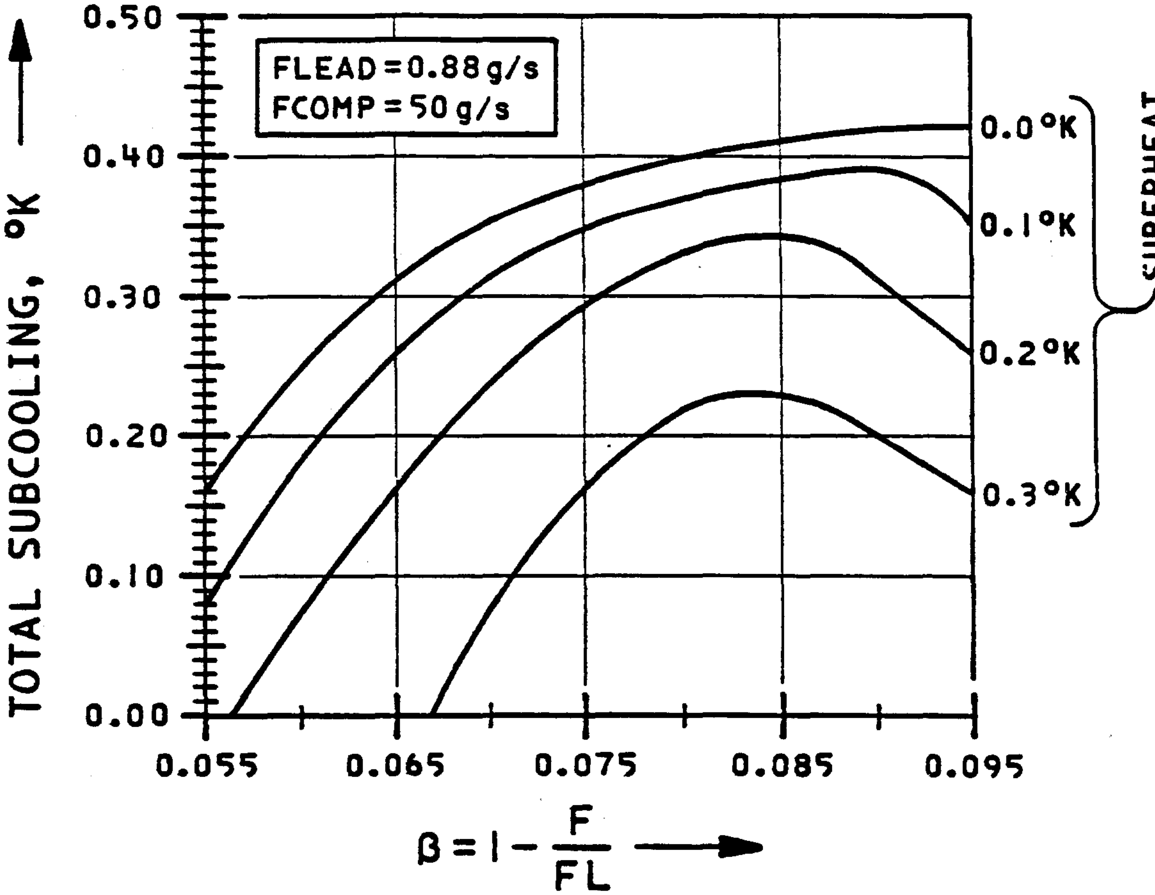
FLEAD = 0.88 g/s
FCOMP = 50 g/s
TOTAL SUBCOOLING, °K
0.50
0.40
0.30
0.20
0.10
0.00
0.055
0.065
0.075
0.085
0.095
0.0°K
0.1°K
0.2°K
0.3°K
SUPERHEAT
β = 1 − F/FL

FIG. 17

3.6 Summed UA

In the process of generating the cooling curves the UA is calculated for each enthalpy step. The summation of these values, step by step, is listed in the output under Cooling Curve, Summed UA. The listing of these values and the known (i.e., design value) UA of the individual heat exchangers (2-4B) allow determination of the exchanger junction temperature from the cooling curves. Note that the accuracy of this determination depends only on the relative values.

TABLE II

UA Design Values*

	HX 2	HX 3	HX 4A	HX 4B	Total
UA (W/°K)	4,655	6,646	1,430	1,216	13,947
UA_n	0.333	0.477	0.102	0.087	1.0

*CCI Report 370-105 (TM-783), April 1978

The Satellite operating mode requires all heat exchangers to have common high- and low-pressure flows. The normalized UA of Table II can then be used to determine junction temperature (see Figure 18). The β dependence of T2, the temperature at the junction of HX2 and HX3, can be used to directly measure β for a wide range of flows (see Figure 19).

4. CONCLUSIONS

This work is one phase of a continuing effort. Phases two and three will make a similar study of the Satellite refrigerator in the "stand alone" mode, and describe dynamic details of magnet string cooling. The final phase will tie the refrigerator in one or the other mode, to the ramping load.

This study has quantified various aspects of the subject; the Central and Satellite compressor utilization maxima, the temperature of refrigeration minima and parameter sensitivities, not generally addressed before. This report has been written in the hope that the remaining questions and program development can benefit from a broad range of comment and suggestion.

The following is a list of known reservations already on the work list:

1. The resolution to T_R is limited to ≃±10m°K by the accuracy of the temperature subroutines.

2. The subcooler investigation is not specific.

3. The data presented here have been compiled by hand, there are no graphic capabilities -- that's a lot of work.

4. T2 is not in the calculated fluid properties list.

5. Same as 4. for T3, T4, T7, T12 and T13, and β dependence not investigated.

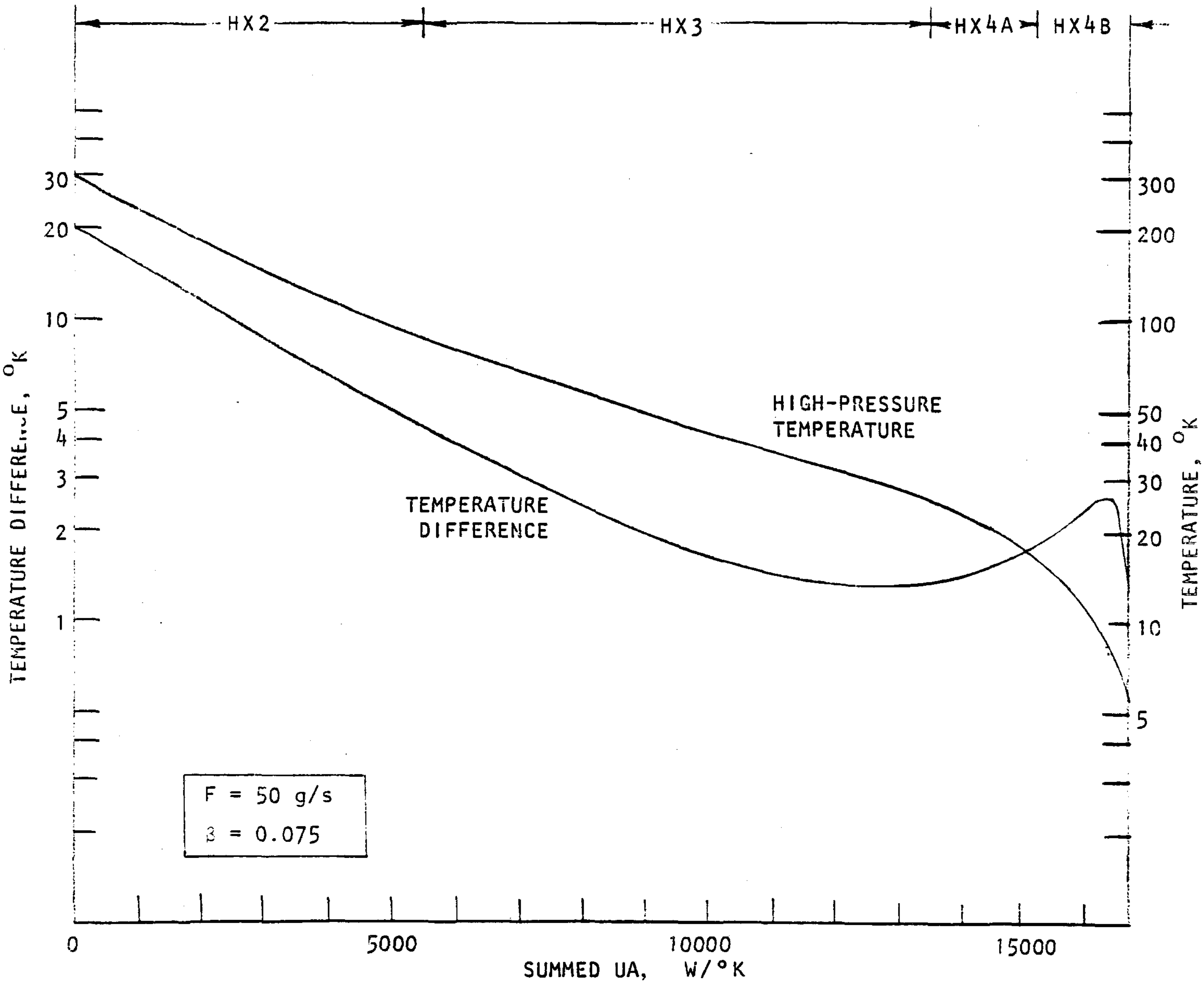
HX2
HX3
HX4A
HX4B
30
20
10
5
4
3
2
1
300
200
100
50
40
30
20
10
5
TEMPERATURE DIFFERENCE, °K
TEMPERATURE, °K
HIGH-PRESSURE TEMPERATURE
TEMPERATURE DIFFERENCE
F = 50 g/s
β = 0.075
0
5000
10000
15000
SUMMED UA, W/°K

FIG. 18

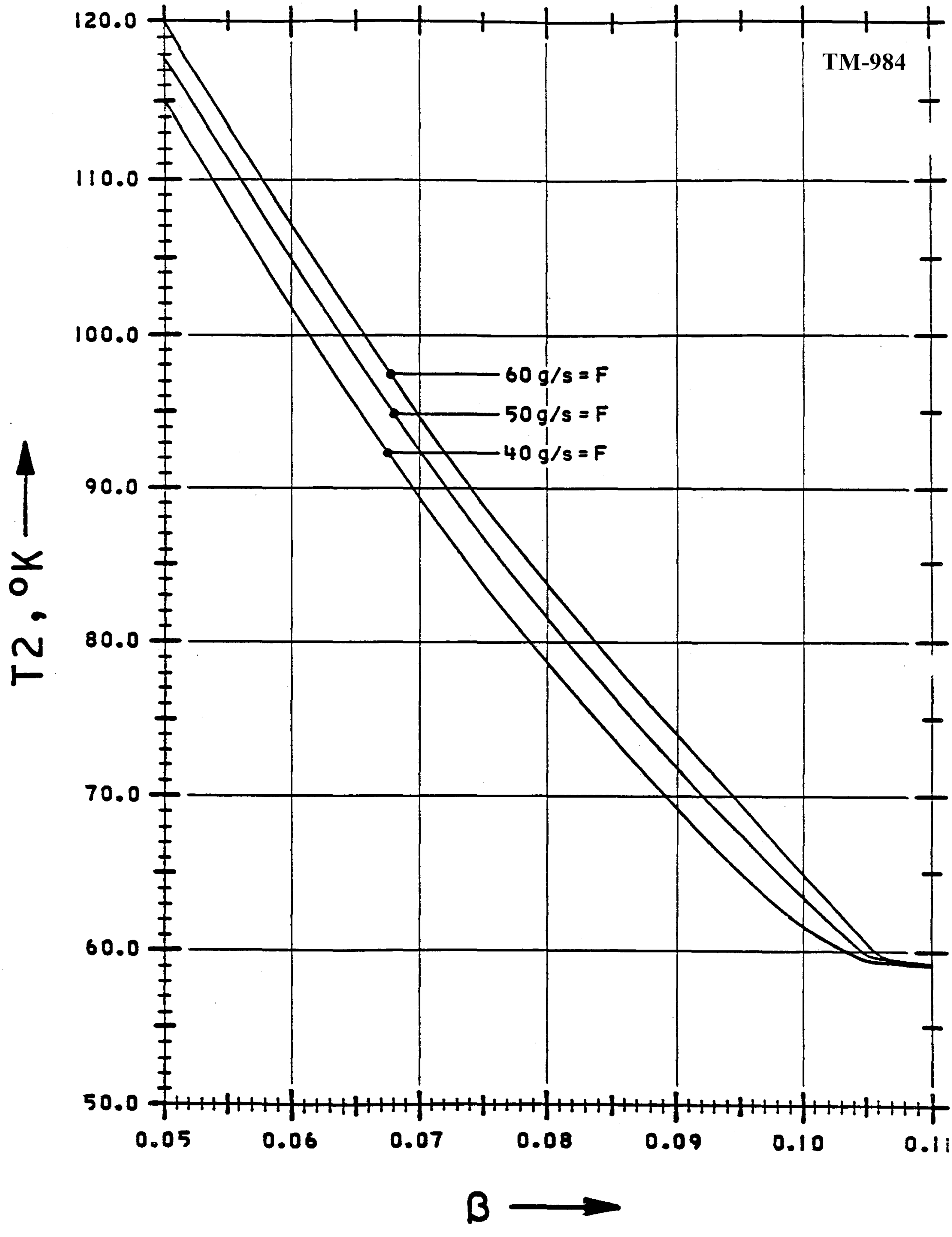
120.0
110.0
100.0
90.0
80.0
70.0
60.0
50.0
T2, °K
60 g/s = F
50 g/s = F
40 g/s = F
0.05
0.06
0.07
0.08
0.09
0.10
0.11
β

FIG. 19

6. Subcooler flow is taken as an even split.

7. High pressure ΔP is taken independent of F.

8. T1 parameter study remains.

9. Compressor efficiency (ECOMP) may not be realistic. This affects overall efficiency determinations and brake horsepower only.

10. The resolution of the Satellite compressor flow optimum in β can be improved -- currently $\approx\pm 0.005$.

11. Refrigeration vs. liquefaction, with β as a parameter, can be extracted from existing data to predict magnet fill rates.

Please call one of the authors with your comments or recommendations for additions to this list.

The program LIQUID can be used from a computer terminal to quickly provide answers to questions about refrigerator performance. The program requires about two seconds of computer time to completely analyze the refrigerator at one operating condition. Interested users will find a program listing, with some comments describing program operation, in the Cryo. Simulation File.

5. ACKNOWLEDGEMENTS

The program LIQUID uses subroutines written at the Cryogenic Division of the National Bureau of Standards to calculate helium properties, and several subroutines obtained from Brookhaven National Laboratory.[3]

The authors are grateful for the assistance of Bert Forester and Stacy Olson who typed the draft of this report, for the illustrations of Bill Cyko, and for the kind cooperation of the Bubble Chamber administration.

---

3. R.King, Determination of the Performance and Cost of the Model 4000 Helium Liquefier, ISABELLE Division Technical Note No. 19, July 23, 1976.